Properties and distribution of paired candidate stony meteorites at Meridiani Planum, Mars

Christian Schröder[1,*], Kenneth E. Herkenhoff[2], William H. Farrand[3], John E. Chappelow[4], Wei Wang[5], Larry R. Nittler[6], James W. Ashley[7], Iris Fleischer[8], Ralf Gellert[9], Matthew P. Golombek[10], Jeffrey R. Johnson[2], Göstar Klingelhöfer[8], Ron Li[5], Richard V. Morris[11], and Steven W. Squyres[12]

[1]University of Bayreuth and Eberhard Karls University of Tübingen, Center for Applied Geoscience, Sigwartstr. 10, 72076 Tübingen, Germany, christian.schroeder@ifg.uni-tuebingen.de

*Corresponding author

[2]Astrogeology Science Center, United States Geological Survey, 2255 N. Gemini Drive, Flagstaff, AZ 86001, USA

[3]Space Science Institute, 4750 Walnut Street, Suite 205, Boulder, CO 80301, USA

[4]SAGA Inc., 1148 Sundance Loop, Fairbanks, AK 99709, USA

[5]Mapping and GIS Laboratory, Department of Civil and Environmental Engineering and Geodetic Science, Ohio State University, 470 Hitchcock Hall, 2070 Neil Avenue, Columbus, OH 43210, USA

[6]Department of Terrestrial Magnetism, Carnegie Institution of Washington, 5241 Broad Branch Road NW, Washington D. C. 20015, USA

[7]Mars Space Flight Facility, School of Earth and Space Exploration, Arizona State University, PO Box 876305, Tempe, AZ 85287, USA

[8]Institut für Anorganische Chemie und Analytische Chemie, Johannes Gutenberg-Universität, Staudinger Weg 9, 55128 Mainz, Germany

[9]Department of Physics, University of Guelph, Guelph, Ontario, N1G 2W1, Canada

[10]Jet Propulsion Laboratory, California Institute of Technology, Mail Stop 183-501, 4800 Oak Grove Drive, Pasadena, CA 91109, USA

[11]NASA Johnson Space Center, ARES Mail Code KR, 2101 NASA Parkway, Houston, TX 77058, USA

[12]Department of Astronomy, Space Sciences Building, Cornell University, 428 Space Sciences, Ithaca, NY 14853, USA

Abstract

The Mars Exploration Rover (MER) Opportunity investigated four rocks, informally dubbed Barberton, Santa Catarina, Santorini and Kasos, that are possible stony meteorites. Their chemical and mineralogical composition is similar to the howardite-eucrite-diogenite group but with additional metal, similar to mesosiderite silicate clasts. Because of their virtually identical composition and because they appear to represent a relatively rare group of meteorites, they are probably paired. The four rocks were investigated serendipitously several kilometers apart, suggesting that Opportunity is driving across a larger population of similar rock fragments, maybe a meteorite strewn field. Small amounts of ferric Fe are a result of weathering. We did not observe evidence for fusion crusts. Four iron meteorites were found across the same area. Although mesosiderites are stony irons, a genetic link to these irons is unlikely. The stony meteorites probably fell later then the irons. The current atmosphere is sufficiently dense to land such meteorites at shallow entry angles, and it would disperse fragments over several kilometers upon atmospheric breakup. Alternatively, dispersion by spallation from an impacting meteoroid may have occurred. Santa Catarina and a large accumulation of similar rocks were found at the rim of Victoria crater. It is possible that they are associated with the impactor that created Victoria crater, but our limited knowledge about their distribution cannot exclude mere coincidence.

1 Introduction

The Mars Exploration Rover (MER) Opportunity landed at Meridiani Planum in January 2004 and has since been driving across terrain dominated by S-rich outcrop rocks, basaltic sand and a hematite lag [e.g., *Morris et al.*, 2006; *Squyres et al.*, 2004, 2006a, 2006b, 2009]. Loose rock fragments scattered across the surface provide the only access to other types of material. The diverse origins of these "cobbles", a term informally used by the MER team to describe any loose rock fragment > 1 cm, are discussed by *Jolliff et al.* [2006] and *Fleischer et al.* [2010c]. Among these cobbles are several meteorites [*Schröder et al.*, 2006, 2008, 2009a]. To date, Opportunity has discovered four iron meteorites and four rocks have been identified as possible stony meteorites on the basis of their chemical and mineralogical composition. The iron meteorites are discussed in detail elsewhere [*Schröder et al.*, 2008; *Fleischer et al.*, 2010a, 2010b; *Ashley et al.*, 2010; *Chappelow et al.*, 2010]. The candidate stony meteorites are the topic of this paper. Surprisingly, although they were investigated serendipitously kilometers apart from each other, they are chemically and mineralogically so similar to each other that we conclude that they are probably paired [*Schröder et al.*, 2009b]. We describe their properties and distribution, lay out the argument for their pairing in detail, and discuss other resulting implications.

2 Methods

Opportunity is equipped with the Athena Science Payload [*Squyres et al.*, 2003]. The apertures of two remote sensing instruments, a 0.27 mrad/pixel, multiple filter visible to near-infrared (400 to 1010 nm) Panoramic camera (Pancam) [*Bell et al.*, 2003] and a Mini-Thermal Emission Spectrometer (Mini-TES) covering the 5 to 29 µm wavelength region [*Christensen et al.*, 2003], are located on top of the Pancam Mast Assembly (PMA). Four contact or in situ

instruments are located at the end of the rover's robotic arm, which is also referred to as Instrument Deployment Device (IDD): a 31 µm/pixel Microscopic Imager (MI) [*Herkenhoff et al.*, 2003], an Alpha Particle X-ray Spectrometer (APXS) for elemental composition [*Rieder et al.*, 2003], a Mössbauer (MB) spectrometer for determining mineralogy of iron-bearing phases, distribution of Fe among those phases, and iron oxidation states [*Klingelhöfer et al.*, 2003], and a Rock Abrasion Tool (RAT) to remove surface contamination and weathering rinds from rock surfaces [*Gorevan et al.*, 2003]. The rovers also carry magnets for attracting dust particles [*Madsen et al.*, 2003], and engineering cameras to support mobility, navigation, science, and placement of the instrument arm [*Maki et al.*, 2003].

To understand the results and discussion below it is important to note that the Field Of View (FOV) of the APXS is ~3 cm. The FOV increases if the instrument is not in contact with the target to be analyzed, but hovers at a certain distance away in order to avoid damage of the detectors from protruding small rocks or outcrop edges. The FOV of the MB is ~1.5 cm.

The MB simultaneously obtains spectra from resonantly absorbed and reemitted 14.4 keV γ-rays and from 6.4 keV X-rays. The different energies result in different attenuation in the target material and hence the comparison of these spectra yields a certain depth selectivity [*Klingelhöfer et al.*, 2003; *Fleischer et al.*, 2008a].

The MB quantifies the Fe-bearing mineralogy of a target as subspectral areas, which are proportional to the relative Fe content of specific mineral phases [e.g., *Morris et al.*, 2006, 2008]. If other elements substitute for Fe, for example Mg in the mineral olivine $(Mg,Fe)_2SiO_4$, the extent of substitution has to be known in order to calculate mineral weight percentages from area ratios. *McSween et al.* [2008] describe how to reconcile MB, APXS and Mini-TES datasets.

Individual MI images and mosaics of MI frames were merged with Pancam color observations, using the techniques described by *Herkenhoff et al.* [2006]. Pancam L2 (753 nm), L5 (535 nm), and L7 (432 nm) images were used for each of these merges and enhanced to emphasize false-color variations.

3 Results

3.1 Physical properties of candidate meteorites

Figure 1 shows the four candidate meteorites encountered by Opportunity. They were dubbed Barberton, Santa Catarina, Santorini and Kasos by the MER team. Note that the place names used in this paper for landforms, rocks, and soils have not been approved by the International Astronomical Union and are meant to be informal and convenient ways to remember features (e.g., an outcrop or aeolian bed form) and targets (e.g., specific location on a feature for which in situ measurements were acquired).

Barberton is located on the rim of Endurance crater (Figure 2) and was investigated on sol 121 of Opportunity's mission. It has already been described in detail by *Schröder et al.* [2006, 2008]. It measures ~3 cm in diameter and is relatively dusty compared to the other three meteorite candidates (Figure 3). Assuming a density between the average density of howardites (2.83 g/cm^3 [*Britt et al.*, 2010]) and ordinary chondrites (3.5 g/cm^3 [*Wilkison and Robinson*, 2000]) and approximating the shape of Barberton as a half sphere with radius 1.5 cm, we estimate its mass between 20 and 25 g. Barberton was too small to be brushed clean of dust with the RAT.

Santa Catarina was discovered on the Cabo Anonimo promontory at the rim of Victoria crater (Figure 2). It was chosen out of an extended field of cobbles at that location for detailed investigation with Opportunity's in situ instruments between sols 1034 and 1055. Santa Catarina was described in detail previously by *Schröder et al.* [2008]. It measures ~14 cm in its longest dimension and ~11 cm across. Approximating its shape with an ellipsoid with semi-principal radii of 7 cm, 5.5 cm and 5.5 cm, respectively, the mass of Santa Catarina is estimated between 2.5 and 3.1 kg. Santa Catarina is a brecciated rock with several subangular clasts clearly visible in MI images (Figure 4; compare also Figure 11 by *Schröder et al.* [2008]). An unfavorable geometry prevented RAT-brushing of its surface.

Santorini is located on the plains of Meridiani Planum ~800 m south of Victoria crater (Figure 2) and was investigated between sols 1713 and 1749 [*Schröder et al.*, 2009a]. Santorini measures approximately 8 × 6 cm. Approximating its shape with an ellipsoid of semi-principal radii of 4 cm, 3cm and 3 cm, respectively, Santorini's mass is estimated between 427 g and 528 g. Because of the brecciated nature of Santa Catarina, two separate spots were investigated on Santorini with the APXS to probe for inhomogeneities in its elemental composition. The two spots were virtually identical (see below and Table 1), consistent with the MI images which reveal a more uniform texture at centimeter scale relative to Santa Catarina (Figure 5). The top of the rock shows a relatively high reflectance, with a glassy, reflective luster on that part of the surface. The top of the cobble appears cleaner than other, dust-covered areas. Again, the rock could not be RAT-brushed because of an unfavorable geometry.

Kasos is located on the plains almost 3 km south of Victoria crater (Figure 2). It was investigated between sols 1884 and 1890 and measures approximately 7 × 6 cm. Approximating Kasos' shape with an ellipsoid with semi-principal radii of 3.5 cm, 3 cm and 3

cm, its mass is estimated between 373 g and 462 g. MI images show a rougher surface compared to Santa Catarina (Figure 6), but also a glassy luster. Few grains or clasts are visible in the MI observations, and color variations are subtle, apparently caused by variations in dust abundance on the surface of the cobble. Again the surface could not be RAT-brushed, but it appears to be relatively free from dust.

3.2 Chemical composition of candidate meteorites

The candidate meteorites are very similar in their elemental composition and form a distinct group among all cobbles investigated by Opportunity (Table 1 and Figure 7). *Fleischer et al.* [2010c] discuss the differences between different sets of cobbles in more detail and draw conclusions on their diverse origin. They refer to the candidate meteorites as Barberton Group cobbles and show that the group is compositionally distinct from other martian materials, including the martian meteorites collected on Earth. The Barberton group cobbles have very high Ni contents, the highest measured to date by either Mars Exploration Rover, Spirit or Opportunity, with the exception of the iron meteorites. Other distinguishing features include high Mg and Cr, and low Al, K and Ti.

The composition of Barberton deviates the most from the otherwise virtually identical compositions of Santa Catarina, Santorini and Kasos. Because of its relatively small size, Barberton did not completely fill the field of view of the APXS instrument, which included surrounding soil. Subtracting a soil component results in a composition much closer to that of the other three candidate meteorites (Table 1, cf. *Schröder et al.* [2008]).

3.3 Fe Mineralogical composition of candidate meteorites

The four candidate meteorites also share the same Fe-bearing mineralogical composition (Table 2). Mössbauer spectra (Figure 8) are dominated by ferrous iron in the minerals olivine

and pyroxene. They are distinct from other martian materials through minor metallic Fe-Ni (kamacite) and troilite phases. All four meteorites further contain some ferric iron as not further-specified nanophase ferric oxide (npOx), which may be any combination of superparamagnetic hematite and goethite, lepidocrocite, ferrihydrite, schwertmannite, akaganéite, hisingerite, and the oct-Fe^{3+} rich particles that pigment iddingsite and palagonite [e.g., *Morris et al.* 2006, 2008]. The ratios of individual mineral phases vary somewhat. Some heterogeneity is not unexpected considering that at least Santa Catarinahas a brecciatedtexture (Figure 4). The Fe-bearing olivine content is larger than pyroxene except for Kasos. The troilite content is larger than kamacite except for Barberton.

4 Discussion

4.1 Grouping of candidate meteorites

The high Ni contents, in combination with metallic iron in the form of kamacite and the sulfide troilite identified in Barberton, Santa Catarina, Santorini and Kasos, provide evidence for their origin as stony meteorites [*Schröder et al.*, 2006, 2008, 2009a]. With limited elemental datasets and in the absence of oxygen isotope data, element ratio plots can be used to distinguish between certain groups of meteorites [*Nittler et al.*, 2004]. Such plots are shown in Figure 9. Barberton, Santa Catarina, Santorini and Kasos plot close to the boundary between howardites and diogenites of the howardite-eucrite-diogenite (HED) group of meteorites. Additional metal (Figures 9a and 9d) led to their possible grouping as mesosiderite silicate clasts [*Schröder et al.*, 2006, 2008], but it is also possible that the four candidate meteorites simply extend the howardite-diogenite range or that they constitute a new group of meteorites not sampled on Earth.

Modal abundances of olivine in mesosiderites are typically much less than those of pyroxene [*Powell*, 1970; *Prinz et al.*, 1980] but, as discussed already by *Schröder et al.* [2008], centimeter-sized olivine clasts have been observed in several mesosiderites [*Boesenberg et al.*, 1997; *Delaney et al.*, 1980; *McCall*, 1966; *Mittlefehldt*, 1980; *Nehru et al.*, 1980] and a thin section of the meteorite MIL03443, tentatively classified as a clast from a mesosiderite, shows a groundmass of coarse comminuted olivine [*McCoy*, 2006].

Bulk mesosiderites contain subequal amounts of metal and silicate and such a rock has not been observed on Mars to date. However, *Schröder et al.* [2008] calculated that the modal amount of metal in Barberton falls in the range of metal modal abundances for several clasts and the whole enclave of an olivine-orthopyroxenite monomict breccia determined by *Kimura et al.* [1991] in the Vaca Muerta mesosiderite.

4.2 Pairing of candidate meteorites

Because of their virtually identical chemical and similar mineralogical compositions, and because they belong to a relatively rare group of meteorites (i.e. not chondrites), Barberton, Santa Catarina, Santorini and Kasos are probably fragments of the same larger body, and are thus considered paired. The four rocks were investigated serendipitously several kilometers apart from each other (Figure 2), suggesting a larger population of similar rock fragments in this area. They may have accumulated as fragments spalled off a larger parent body upon impact, which may have created one or more of the craters in this area. Alternatively, Opportunity may be driving across a meteorite strewn field.

4.3 Alteration of candidate meteorites – fusion crust or weathering?

The candidate meteorites each contain Fe in metallic (Fe^0), ferrous (Fe^{2+}) and ferric (Fe^{3+}) oxidation states. The ferric Fe is not intrinsic to the meteorites but a product of oxidative alteration since their arrival on Mars.

Passage through the atmosphere at high speeds melts the outermost portion of a meteorite. Most of this melt is ablated. The remainder forms a thin, glassy and shiny, mostly dark (often almost black) fusion crust on stony meteorites. In meteorites found on Earth, this fusion crust contains enhanced amounts of ferric Fe similar to npOx [e.g. *Schröder et al.*, 2004], though it is not clear whether the same would form in Mars' atmosphere, which lacks free oxygen. As an added effect, corners, edges or protuberances tend to be ablated away, resulting in rounded, aerodynamic shapes. Although Santorini appears shiny on parts of its surface (Figures 1c and 5), none of the four candidate meteorites is particularly rounded. A dark fusion crust is not apparent in any of the Pancam or MI images (Figures 1 and 3-6). Furthermore, a thin layer of fusion crust enriched in ferric Fe relative to a ferric-free substrate should give an enhanced signal in 6.4 keV Mössbauer spectra, analogous to the ferric-rich coating on the rock Mazatzal analyzed by MER Spirit in Gusev crater [*Fleischer et al.*, 2008]. At least for Barberton and Santa Catarina, such a signal was not observed [*Fleischer et al.*, 2009], although Santa Catarina has the highest ferric Fe content of the four candidate meteorites. We therefore conclude that the ferric Fe in the four candidate meteorites is not part of a fusion crust, and the visible parts of the rocks do not exhibit any fusion crust.

Hence, the ferric Fe is most likely a product of chemical weathering. *Ashley and Wright* [2004] proposed metallic Fe in meteorites as a sensitive tracer of surface-volatile interactions on Mars. The largest amount of ferric iron in the four meteorite candidates was observed in Santa Catarina, which coincides with the smallest amount of metallic Fe. We take this as evidence for interaction with water, either as transient thin films of liquid water or ice or

water vapor, which oxidized the metallic Fe into a ferric phase. Because we only observe npOx, i.e. paramagnetic or superparamagnetic iron oxides or hydroxides, this interaction was limited. Larger amounts of or longer exposures to water would have led to the formation of magnetically ordered Fe oxides or hydroxides [*Bland et al.*, 1998].

4.4 Effects of dynamic interactions with the atmosphere

The probability of landing meteorites on the surface of Mars is to first order a function of the thickness of its atmosphere. *Bland and Smith* [2000] found that stony meteoroids of up to ~0.1 kg may be decelerated sufficiently by Mars' current atmosphere to survive impact. Santa Catarina, Santorini and Kasos exceed that limit and one may ask whether a thicker atmosphere at some point in the past was necessary to land those meteorites. However, for simplicity, *Bland and Smith* [2000] explored only vertical incidence, the least favorable entry angle for producing meteorites.

Chappelow and Sharpton [2006a] did not limit their study to any particular entry angle, instead searching across all possible entry angles. They found that stones up to at least 30 kg in mass [cf. Figure 2b in *Chappelow and Sharpton*, 2006a] may be landed under current martian conditions if they enter the atmosphere between roughly 10 and 20 degrees [cf. Figure 3b in *Chappelow and Sharpton*, 2006a]. Thus, it is not necessary to invoke a denser martian atmosphere to account for any of the suspected stony meteorites discovered by Opportunity to date, even if each represents a single, individual fall. Of course sizes and rates of such falls would be higher under a denser atmosphere. Based on modeling results using the methods by *Chappelow and Sharpton* [2006a, 2006b], today's atmosphere should produce many such meteorites, and they should be rather common on Mars; considerably more common than irons of the same size range. Their presence on the surface says little about what martian

atmospheric conditions may have prevailed when they landed, from an entry and passage dynamics point of view.

Under the current martian atmosphere (~6 mbar surface pressure), the original meteoroids are essentially limited to entry velocities less than ~17 km s^{-1}, and greater than the minimum of ~6 km s^{-1} (Figure 10), and entry angles greater than 8° and less than 39° (at 100 km altitude). While these limits seem constrictive, according to the entry velocity distribution used by *Chappelow and Sharpton* [2006a] and the usual cosine-squared entry angle distribution, about one third of all Mars-incident meteoroids fall within this range. Therefore, stony-type meteorites in this mass range should not be uncommon on Mars.

There is a possibility that stony meteorites may fragment under the dynamic pressure of high speed passage through the atmosphere; indeed the shapes of these meteorites, their apparent lack of fusion crusts and their proximity to each other argue for the possibility that they are the result of such an event, and therefore constitute parts of a meteorite strewn field. Although the computer model of *Chappelow and Sharpton* [2006a, 2006b] used herein does not explicitly treat fragmentation, much information can be obtained from the results it does yield. For example, the differences in masses between various test objects results in differences in their deceleration resulting from air drag. This differential drag deceleration causes larger stones to fall further downrange than smaller ones, and it is one of the effects that cause the scatter of the fragments of meteoroids which fragment in any atmosphere. Results of the simulations indicate that the downrange distance differences among test objects with the same velocity and entry angle, but different masses are commonly tens or even hundreds of kilometers. Thus separation by differential drag alone is sufficient to explain the scatter of the stones found on Mars, and there is no dynamical reason to rule out the possibility that the Barberton Group cobbles may represent a strewn field. A primary reason for these large

separation distances is their very long flight paths which are the result of the shallow entry angles required for the meteorites to survive impact.

However, another modeling result is that the test meteoroids do not encounter dynamic pressures great enough to fragment them, unless they are assumed to be extremely weak, for example, because of preexisting fractures. Maximum dynamic pressures of a few MPa are typical, which is between one and two orders of magnitude smaller than the estimated compressive strengths of small stony meteorites (tens to hundreds of MPa [*Petrovich*, 2001]). While the dynamic pressures encountered are higher for steeper entry angles, such entry angles result in much shorter flight paths which do not favor meteorite survival or fragment spreading. Thus strewn fields may be rather rare for these types of meteorites.

Masses of test meteoroids were limited to 10 kg. Meteoroids with larger mass would be faster when reaching the denser lower atmosphere, and larger objects tend to be weaker than smaller ones, increasing the probability of fragmentation. On the other hand, larger speeds would limit the separation by differential drag. It is therefore unclear whether meteoroids large enough to fragment in the atmosphere can be dispersed across distances similar to the ones observed for the Barberton Group cobbles

4.5 Relationship to Victoria crater

Victoria crater has been the subject of extensive exploration by Opportunity [*Squyres et al.*, 2009]. Because Santa Catarina was found at its rim, it is tempting to hypothesize a relationship between Santa Catarina and the formation of Victoria crater.

Santa Catarina was chosen for detailed investigation with the rover's contact instruments out of an extended field of cobbles, 96 m x 108 m as visible from the rover [*Schröder et al.*,

2008], scattered on the Cabo Anonimo promontory at the rim of Victoria crater. At least several of the remaining cobbles have the same composition on the basis of Pancam 13 filter and Mini-TES spectral observations [*Schröder et al.*, 2008; *Ashley et al.*, 2009a]. Hence, the largest accumulation of Barberton Group cobbles was observed at the rim of Victoria crater. Barberton to the north of Victoria and Santorini and Kasos to the south of Victoria are located at distances comparable to the distances from the crater rim at which fragments of the Canyon Diablo meteorite that created Barringer Meteorite Crater in Arizona were discovered (compare Figures 11 and 12). Note that Canyon Diablo is a IAB complex iron meteorite, not a stony meteorite. Barringer Meteor Crater has a diameter of 1.2 km whereas Victoria crater's diameter is ~750 m [*Squyres et al.*, 2009].

Because 1) the largest observed accumulation of rock fragments of this kind is at the rim of Victoria; 2) the largest fragment investigated (Santa Catarina) is located at the rim of Victoria, and the smallest investigated fragment (Barberton) is located furthest from Victoria; 3) the population as a whole appears to surround Victoria; 4) the four candidate meteorites show no obvious signs of a fusion crust in Pancam or MI images nor any ablation features (Figures 1 and 3-6), which may be taken as evidence that they are spalled-off fragments of an impactor; and 5) our simulations showed that atmospheric break-up of the parent meteoroid is a small probability event, it appears possible that Barberton, Santa Catarina, Santorini and Kasos are associated in some way with the impactor that created Victoria crater.

However, we do not know the complete extent and distribution of Barberton Group cobbles at Meridiani Planum. This plus the statistically small number of Barberton Group cobbles investigated in detail casts some uncertainty on the above-drawn conclusion. The path of the Opportunity rover to and from Victoria crater was not random and may not be a representative sample of the terrain: For the most part, Opportunity tended to drive down large troughs in

order to stay clear of large ripples which might have impeded motion. This style of traverse may have limited our view of other significant cobble accumulations.

Although Opportunity circumnavigated approximately half of Victoria crater, why did we see a large accumulation of cobbles, the Santa Catarina cobble field, only at its northern rim? The Victoria annulus is very flat and relatively free of debris, affording an unobstructed view in all directions. *Grant et al.* [2008] estimate ~1 m of deflation of the annulus by aeolian erosion. Any of the meteorite candidates would arguably be more resistant to this kind of erosion than the underlying S-rich outcrop rocks. So why do we not see many more cobbles around Victoria if the Barberton Group cobbles are fragments of the Victoria impactor?

As the example of Barringer Meteorite Crater shows, fragments of the impactor are not evenly distributed but cluster mainly at the northeastern part of the rim (Figure 12). Aeolian actions may not only expose potential meteorite fragments by deflation, but may also bury them through ripple migration or wind-blown dust accumulations in other places. If the Barberton Group cobbles were unrelated to the formation of Victoria and fell later, a strewn field would not necessarily stop at the crater rim. Thus, finding a fragment on the floor of Victoria would argue against this hypothesis. No cobbles were observed in Pancam images of the crater floor, but the crater floor was relatively distant and *Grant et al.* [2008] estimate ~50 m of infilling by sediments. Opportunity cautiously entered the crater at Duck Bay [*Squyres et al.*, 2009]. A cobble on the slopes of Duck Bay, dubbed Jin, was scheduled for detailed investigation that was eventually precluded by rover mobility constraints. However, these results would have been inconclusive anyway because backwasting widened the crater by approximately 150 m [*Grant et al.*, 2008] and the cobble could have been on top of the original rim of Victoria. This backwasting may have also obscured other accumulations at the original crater rim.

Given our poor knowledge of the total distribution of this group of stony meteorite candidates and their uneven distribution on the annulus of Victoria crater, we cannot distinguish their originating from the Victoria crater impact versus some other impact either before or after the Victoria impact.

4.6 Relationship to iron meteorites

Four iron meteorites were discovered by Opportunity: Heat Shield Rock a.k.a. Meridiani Planum [*Schröder et al.*, 2008; *Fleischer et al.*, 2010b], Block Island, Shelter Island, and Mackinac Island [*Fleischer et al.*, 2010a; *Ashley et al.*, 2010; *Chappelow et al.*, 2010; *Gellert et al.*, 2010]. These were encountered across the same distance as the Barberton Group cobbles (Figure 2). Heat Shield Rock is grouped as a IAB complex iron meteorite [*Schröder et al.*, 2008] as are at least two of the other three irons (Gellert et al., APXS on Iron Nickel Meteorites at Meridiani Planum, Mars, manuscript in preparation); Mackinac Island was remotely imaged only and not analyzed with the IDD instruments. On the basis of the chemical similarity, the iron meteorites may also be paired [*Fleischer et al.*, 2010a], and Opportunity may have been driving across two overlapping strewn fields (Figure 2).

If the four candidate stony meteorites are mesosiderite silicate clasts [*Schröder et al.*, 2006, 2008], one may explore a genetic relationship with the iron meteorites as the missing metal fraction. However, we consider such a relationship unlikely because 1) mesosiderites have been linked to the IIIAB iron meteorite group [*Hassanzadeh et al.*, 1990], not IABs; 2) the irons are probably older than the candidate stony meteorites (see section 4.7); and 3) the geochemical argument for pairing of the Meridiani irons is weaker than the case for the stones.

Although IAB irons make up only 1 % of falls on Earth, they make up 15 % among irons only [*Grady*, 2000] and are thus not a rare group. The four irons on Meridiani are very close in their chemical composition, and although IAB iron compositions show a large variability in Ge-Ni plots, they are within the composition most common for IABs. There are large variations between the four irons in their degree of alteration on the basis of morphological features [*Ashley et al.*, 2010], and hence they might have fallen at different times.

4.7 Relative age of candidate stony meteorites

The irons differ from the candidate stony meteorites in their degree of alteration. Because of their close proximity (Figure 2) they must have fallen at different times in order to have experienced different weathering regimes. All four iron meteorites display discontinuous "purple" (in false-color Pancam imagery) coatings on their surface [cf. Figure 4 in *Schröder et al.*, 2008; *Johnson et al.*, 2010], which are not observed on any of the stony meteorite candidates (Figures 1 and 3-6). These coatings are likely the result of chemical weathering, perhaps partially eroded by aeolian abrasion, rather than a remnant fusion crust [*Johnson et al.*, 2010; *Ashley et al.*, 2010]. *Fleischer et al.* [2010b] have identified small amounts of magnetically ordered Fe oxides in Heat Shield Rock. This argues for enhanced chemical weathering relative to the stony meteorites (cf. section 4.3) and therefore greater ages. On the other hand, the same environmental conditions that resulted in those coatings on a metallic Fe substrate would not necessarily lead to the same or similar coating on a silicate substrate.

The iron meteorites do not contain any visible mineral inclusions but some of the pits may be the result of preferential weathering, chemically or mechanically, of minerals such as troilite and possibly silicates such as olivine [*Ashley et al.*, 2010]. *Ashley et al.* [2010] also show delicate metal protrusions in the iron meteorite Block Island, which would not have survived passage through Mars' atmosphere or landing and are therefore evidence for the subsequent

removal of mineral inclusions by preferential weathering. The four stony meteorite candidates, on the other hand, have a large amount of the Fe in olivine and pyroxene and still contain troilite. The irons therefore are probably older than the candidate stony meteorites.

Bland and Smith [2000] estimate that meteorites may survive on Mars' surface for billions of years. Below we list ages relevant for the meteorites encountered by Opportunity, but we cannot conclusively constrain absolute ages for either the irons nor the candidate stony meteorites. The presence of hematite-rich spherules in hollows indicates that the irons were buried by ripples migrating over them at least once [*Ashley et al.*, 2010]. Ripple migration at Meridiani ceased ~100 ka ago [*Golombek et al.*, 2010]. The population of relatively fresh craters on Meridiani yields a model crater isochron age of about 10 Ma [*Lane et al.*, 2003; *Golombek et al.*, 2010], which can be applied as an estimate of the age of Victoria crater. A lag of hematite-rich spherules eroding out of the underlying S-rich outcrop has accumulated on top of basaltic sands at Meridiani [e.g., *Soderblom et al.*, 2004]. Comparing the average volume concentration of these spherules in outcrop and in the top centimeter of basaltic sand, *Golombek et al.* [2006] calculated 10 to 50 cm of erosion in the Late Amazonian (since ~0.4 Ga). One of the iron meteorites, Block Island, sits on a 4 cm-high pedestal of S-rich outcrop [*Ashley et al.*, 2010]. The depth of its original emplacement in or on the S-rich outcrop and overlying sand is unknown. The S-rich outcrops themselves are of late Noachian age (before 3.5 Ga) [*Arvidson et al.*, 2006].

5 Conclusions

The four rocks Barberton, Santa Catarina, Santorini and Kasos are a distinct group of rocks on Meridiani Planum on the basis of their elemental and mineralogical composition. Their high Ni contents as well as the minerals kamacite and troilite suggest a meteoritic origin. Their

composition is similar to howardites and diogenites, but with additional metal. Therefore, they have been suggested to be similar to mesosiderite silicate clasts, but they may also represent a new group of meteorites or simply extend the known compositional range of howardites and diogenites. In any case, they are not chondritic and therefore belong to a relatively rare group of meteorites. This together with their virtually identical chemical and very similar mineralogical composition led us to the conclusion that the four Barberton Group cobbles are paired meteorites.

Ferric Fe in the meteorites is a result of weathering, probably oxidation of the Fe metal phase, and not the formation of an oxidative fusion crust. We see no other evidence for a fusion crust, which suggests that they fragmented during passage through the atmosphere or that they are fragments spalled off a crater-forming meteoroid upon impact.

The four meteorite rocks were investigated serendipitously over a distance of ~10 km, suggesting a larger population of such fragments in the area and that Opportunity may be driving across a meteorite strewn field. The current martian atmosphere is sufficient to land and disperse these meteorites across such a distance if they enter the atmosphere at shallow angles. However, dynamic pressures experienced by meteoroids passing through the current atmosphere at such angles are generally too low to result in fragmentation. Spallation from an impactor may thus be the more likely explanation for the dispersion of the four candidate meteorites. Because Santa Catarina and an accumulation of similar rock fragments were discovered at the rim of Victoria crater, it is possible that the meteorite candidates are associated with the impactor that created Victoria. We cannot exclude mere coincidence, however, given our limited knowledge of the distribution of these rocks.

Mesosiderites have a genetic relationship to iron meteorites. Opportunity also discovered four iron meteorites across the same distance as the four stony meteorite candidates. A genetic link between these irons and stones appears unlikely on the basis of their different stages of weathering, however. The stones probably fell later than the irons, but we cannot constrain absolute ages.

Acknowledgements

We thank David Kring for his permission to show the map of distribution of meteoritic material around Meteor Crater reproduced in Figure 12. We acknowledge the unwavering support of JPL engineering and MER operations staff and the MER Athena Science Team.

References

Arvidson, R. E., F. Poulet, R. V. Morris, J.-P. Bibring, J. F. Bell III, S. W. Squyres, P. R. Christensen, G. Bellucci, B. Gondet, B. L. Ehlmann, W. H. Farrand, R. L. Fergason, M. Golombek, J. L. Griffes, J. Grotzinger, E. A. Guinness, K. E. Herkenhoff, J. R. Johnson, G. Klingelhöfer, Y. Langevin, D. Ming, K. Seelos, R. J. Sullivan, J. G. Ward, S. M. Wiseman, and M. Wolff (2006), Nature and origin of the hematite-bearing plains of Terra Meridiani based on analyses of orbital and Mars Exploration rover data sets, *J. Geophys. Res.*, *111*, E12S08, doi:10.1029/2006JE002728.

Ashley, J. W., and S. P. Wright (2004), Iron oxidation products in Martian ordinary chondrite finds as possible indicators of water exposure at Mars Exploration Rover landing sites, *Lunar Planet. Sci.*, *35*, 1750.

Ashley, J. W., S. W. Ruff, A. T. Knudson, and P. R. Christensen (2009a), Mini-TES measurements of Santa Catarina-type, stony-iron meteorite candidates by the Opportunity rover, *Lunar Planet. Sci.*, *40*, 2468.

Ashley, J. W., M. P. Golombek, P. R. Christensen, I. Fleischer, K. E. Herkenhoff, J. R. Johnson, T. J. McCoy, T. J. Parker, C. Schröder, S. W. Squyres, and the Athena Science Team (2010), Evidence for Mechanical and Chemical Alteration of Three New Iron-Nickel Meteorites on Mars – Process Insights for Meridiani Planum, *J. Geophys. Res.*, manuscript 2010JE003672, in review.

Bell, J. F., III, S. W. Squyres, K. E. Herkenhoff, J. N. Maki, H. M. Arneson, D. Brown, S. A. Collins, A. Dingizian, S. T. Elliot, E. C. Hagerott, A. G. Hayes, M. J. Johnson, J. R. Johnson, J. Joseph, K. Kinch, M. T. Lemmon, R. V. Morris, L. Scherr, M. Schwochert, M. K. Shepard, G. H. Smith, J. N. Sohl-Dickstein, R. J. Sullivan, W. T. Sullivan, and M. Wadsworth (2003), Mars Exploration Rover Athena Panoramic Camera (Pancam) investigation, *J. Geophys. Res.*, *108*(E11), 8063, doi:10.1029/2003JE002070.

Bland, P. A., and T. B. Smith (2000), Meteorite Accumulations on Mars, *Icarus*, *144*, 21-26, doi:10.1006/icar.1999.6253.

Bland, P. A., A. S. Sexton, A. J. T. Jull, A. W. R. Bevan, F. J. Berry, D. M. Thornley, T. R. Astin, D. T. Britt, and C. T. Pillinger (1998), Climate and rock weathering: A study of terrestrial age dated ordinary chondritic meteorites from hot desert regions, *Geochim. Cosmochim. Acta*, *62*, 3169-3184.

Boesenberg, J. S., J. S. Delaney, and M. Prinz (1997), Magnesian megacrysts and matrix in the mesosiderite Lamont, *Lunar Planet. Sci., 37*, 1491.

Britt, D. T., R. J. Macke, W. Kiefer, and G. J. Consolmagno (2010), An overview of achondrite density, porosity and magnetic susceptibility, *Lunar Planet. Sci., 41*, 1869.

Chappelow, J. E., and V. L. Sharpton (2006a), Atmospheric variations and meteorite production on Mars, *Icarus*, *184*, 424-435.

Chappelow, J. E., and V. L. Sharpton (2006b), The event that produced heat shield rock and its implications for the Martian atmosphere, *Geophys. Res. Lett., 33*, L19201, doi:10.1029/2006GL027556.

Chappelow, J., M. P. Golombek et al. (2010), Entry and landing conditions that produced Block Island, *J. Geophys. Res.*, in review.

Christensen, P. R., G. L. Mehall, S. H. Silverman, S. Anwar, G. Cannon, N. Gorelick, R. Kheen, T. Tourville, D. Bates, S. Ferry, T. Fortuna, J. Jeffryes, W. O'Donnell, R. Peralta, T. Wolverton, D. Blaney, R. Denise, J. Rademacher, R. V. Morris, and S. W. Squyres (2003), Miniature Thermal Emission Spectrometer for the Mars Exploration Rovers, *J. Geophys. Res., 108*(E12), 8064, doi:10.1029/2003JE002117.

Delaney, J. S., and C. E. Nehru (1980), Olivine clasts from mesosiderites and howardites: Clues to the nature of achondrite parent bodies, *Proc. Lunar Planet. Sci. Conf. 11th*, 1073–1087.

Fleischer, I., G. Klingelhöfer, C. Schröder, R. V. Morris, M. Hahn, D. Rodionov, R. Gellert, and P. A. de Souza Jr. (2008a), Depth selective Mössbauer Spectroscopy: Analysis and simulation of 6.4 keV and 14.4 keV spectra obtained from rocks at Gusev crater, Mars, and layered laboratory samples, *J. Geophys. Res.*, *113*, E06S21, doi:10.1029/2007JE003022.

Fleischer, I., G. Klingelhöfer, R. V. Morris, C. Schröder, D. Rodionov, and P. de Souza (2008b), Analysis of 6.4 keV Mössbauer Spectra Obtained with MIMOS II on MER on Cobbles at Meridiani Planum, Mars and Considerations on Penetration Depths, *Lunar Planet. Sci.*, *39*, 1618.

Fleischer, I., G. Klingelhöfer, C. Schröder, D. W. Mittlefehldt, R. V. Morris, M. Golombek, and J. W. Ashley (2010a), In situ investigation of iron meteorites at Meridiani Planum, Mars, *Lunar Planet. Sci.*, *41*, 1791.

Fleischer, I., C. Schröder, G. Klingelhöfer, J. Zipfel, R. V. Morris, J. W. Ashley, and R. Gellert (2010b), New insights into the mineralogy and weathering of the Meridiani Planum Meteorite, Mars: Identification of kamacite, taenite, schreibersite, and iron oxides, *Meteorit. Planet. Sci.*, in review.

Fleischer, I., G. Klingelhöfer, W. H. Farrand, E. Treguier, K. E. Herkenhoff, J. W. Ashley, C. Schröder, C. Weitz, B. L. Jolliff,, S. W. Squyres, J. R. Johnson, J. Brückner, D. W. Mittlefehldt, M. P. Golombek, R. V. Morris, R. Gellert, and P. A. de Souza Jr. (2010c), Mineralogy and Chemistry of Cobbles at Meridiani Planum, Mars, *J. Geophys. Res.*, manuscript 2010JE003621, in review.

Golombek, M. P., J. A. Grant, L. S. Crumpler, R. Greeley, R. E. Arvidson, J. F. Bell III, C. M. Weitz, R. Sullivan, P. R. Christensen, L. A. Soderblom, and S. W. Squyres (2006), Erosion rates at the Mars Exploration Rover landing sites and long-term climate change on Mars, *J. Geophys. Res.*, *111*, E12S10, doi:10.1029/2006JE002754.

Golombek, M., K. Robinson, A. McEwen, N. Bridges, B. Ivanov, L. Tornabene, and R. Sullivan (2010), Constraints on Ripple Migration at Meridiani Planum from Opportunity and HiRISE Observations of Fresh Craters, *J. Geophys. Res.*, in review.

Gorevan, S. P., T. Myrick, K. Davis, J. J. Chau, P. Bartlett, S. Mukherjee, R. Anderson, S. W. Squyres, R. E. Arvidson, M. B. Madsen, P. Bertelsen, W. Goetz, C. S. Binau, and L. Richter (2003), Rock Abrasion Tool Mars Exploration Rover Mission, *J. Geophys. Res.*, *108*(E12), 8068, doi:10.1029/2003JE002061.

Grady, M. M. (2000), *Catalogue of Meteorites*, Cambridge University Press, New York.

Grant, J. A., S. A. Wilson, B. A. Cohen, M. P. Golombek, P. E. Geissler, R. J. Sullivan, R. L. Kirk, and T. J. Parker (2008), Degradation of Victoria crater, Mars, *J. Geophys. Res.*, *113*, E11010, doi:10.1029/2008JE003155.

Hassanzadeh, J., A. E. Rubin, and J. T. Wasson (1990), Compositions of large metal nodules in mesosiderites: Links to iron meteorite group IIIAB and the origin of mesosiderite subgroups, *Geochim. Cosmochim. Acta*, *54*, 3197-3208.

Herkenhoff, K., S. W. Squyres, J. F. Bell III, J. N. Maki, H. M. Arneson, P. Bertelsen, D. I. Brown, S. A. Collins, A. Dingizian, S. T. Elliott, W. Goetz, E. C. Hagerott, A. G. Hayes, M.

J. Johnson, R. L. Kirk, S. McLennan, R. V. Morris, L. M. Scherr, M. A. Schwochert, L. R. Shiraishi, G. H. Smith, L. A. Soderblom, J. N. Sohl-Dickstein, and M. V. Wadsworth (2003), Athena Microscopic Imager investigation, *J. Geophys. Res., 108*(E12), 8065, doi:10.1029/2003JE002076.

Herkenhoff, K. E., S. W. Squyres, R. Anderson, B. A. Archimal, R. E. Arvidson, J. M. Barrett, K. J. Becker, J. F. Bell III, C. Budney, N. A. Cabrol, M. G. Chapman, D. Cook, B. L. Ehlmann, J. Farmer, B. Franklin, L. R. Gaddis, D. M. Galuzka, P. A. Garcia, T. M. Hare, E. Howington-Kraus, J. R. Johnson, S. Johnson, K. Kinch, R. L. Kirk, E. Mae Lee, C. Leff, M. Lemmon, M. B. Madsen, J. N. Maki, K. F. Mullins, B. L. Redding, L. Richter, M. R. Rosiek, M. H. Sims, L. A. Soderblom, N. Spanovich, R. Springer, R. M. Sucharski, T. Sucharski, R. Sullivan, J. M. Torson, and A. Yen (2006), Overview of the Microscopic Imager Investigation during Spirit's first 450 sols in Gusev crater, *J. Geophys. Res., 111*, E02S04, doi:10.1029/2005JE002574.

Johnson, J. R., K. E. Herkenhoff, J. F. Bell III, W. H. Farrand, J. Ashley, C. Weitz, and S. W. Squyres (2010), Pancam Visible/Near-Infrared Spectra of Large Fe-Ni Meteorites at Meridiani Planum, Mars, *Lunar Planet. Sci., 41*, 1974.

Jolliff, B. L., W. H. Farrand, J. R. Johnson, C. Schröder, and C. M. Weitz (2006), Origin of rocks and cobbles on the Meridiani Plains as seen by Opportunity, *Lunar Planet. Sci., 37*, 2401.

Kimura, M., Y. Ikeda, M. Ebihara, and M. Prinz (1991), New enclaves in the Vaca Muerta mesosiderite: Petrogenesis and comparison with HED meteorites, *Meteorites, 4*, 263– 306.

Klingelhöfer, G., R. V. Morris, B. Bernhardt, D. Rodionov, P. A. de Souza Jr., S. W. Squyres, J. Foh, E. Kankeleit, U. Bonnes, R. Gellert, C. Schröder, S. Linkin, E. Evlanov, B. Zubkov, and O. Prilutski (2003), Athena MIMOS II Mössbauer spectrometer investigation, *J. Geophys. Res.*, *108*(E12), 8067, doi:10.1029/2003JE002138.

Kring, D. A., *Guidebook to the Geology of Barringer Meteorite Crater, Arizona (a.k.a. Meteor Crater)*, LPI Contribution No. 1355, Lunar and Planetary Institute, Houston, 2007 (available online at http://www.lpi.usra.edu/publications/books/barringer_crater_guidebook/).

Lane, M. D., P. R. Christensen, and W. K. Hartmann (2003), Utilization of the THEMIS visible and infrared imaging data for crater population studies of the Meridiani Planum landing site, *Geophys. Res. Lett.*, *30*(14), 1770, doi:10.1029/2003GL017183.

Li, R. et al. (2010), Rover positioning comparison using orbital and ground positions for both rovers, *J. Geophys. Res.*, this issue, in review.

Madsen, M. B., P. Bertelsen, W. Goetz, C. S. Binau, M. Olsen, F. Folkmann, H. P. Gunnlaugsson, K. M. Kinch, J. M. Knudsen, J. Merrison, P. Nørnberg, S. W. Squyres, A. S. Yen, J. D. Rademacher, S. Gorevan, T. Myrick, and P. Bartlett (2003), Magnetic Properties Experiments on the Mars Exploration Rover mission, *J. Geophys. Res.*, *108*(E12), 8069, doi:10.1029/2002JE002029.

Maki, J. N., J. F. Bell III, K. E. Herkenhoff, S. W. Squyres, A. Kiely, M. Klimesh, M. Schwochert, T. Litwin, R. Willson, A. Johnson, M. Maimone, E. Baumgartner, A. Collins, M. Wadsworth, S. T. Elliot, A. Dingizian, D. Brown, A. C. Hagerott, L. Scherr, R. Deen, D.

Alexander, and J. Lorre (2003), Mars Exploration Rover Engineering Cameras, *J. Geophys. Res.*, *108*(E12), 8071, doi:10.1029/2003JE002077.

McCall, G. J. H. (1966), The petrology of Mount Padbury mesosiderite and its achondrite enclaves, *Mineral. Mag.*, *35*, 1029–1060.

McCoy, T. J. (2006), Thin section description of sample no. MIL 03443, *Antarct. Meteorite Newsl.*, *29*(2), p. 32, JSC Curator's Off., Houston, Tex.

McSween, H. Y., S. W. Ruff, R. V. Morris, R. Gellert, G. Klingelhöfer, P. R. Christensen, T. J. McCoy, A. Ghosh, J. M. Moersch, B. A. Cohen, A. D. Rogers, C. Schröder, S. W. Squyres, J. Crisp, and A. Yen (2008), Mineralogy of volcanic rocks in Gusev crater, Mars: Reconciling Mössbauer, APXS, and Mini-TES spectra, *J. Geophys. Res.*, *113*, E06S04, doi:10.1029/2007JE002970.

Mittlefehldt, D. W. (1980), The composition of mesosiderite olivine clasts and implications for the origin of pallasites, *Earth Planet. Sci. Lett.*, *51*, 29– 40.

Morris, R. V., G. Klingelhöfer, C. Schröder, D. S. Rodionov, A. Yen, D. W. Ming, P. A. de Souza Jr., T. Wdowiak, I. Fleischer, R. Gellert, B. Bernhardt, U. Bonnes, B. A. Cohen, E. N. Evlanov, J. Foh, P. Gütlich, E. Kankeleit, T. McCoy, D. W. Mittlefehldt, F. Renz, M. E. Schmidt, B. Zubkov, S. W. Squyres, and R. E. Arvidson (2006), Mössbauer mineralogy of rock, soil, and dust at Meridiani Planum, Mars: Opportunity's journey across sulfate-rich outcrop, basaltic sand and dust, and hematite lag deposits, *J. Geophys. Res.*, *111*, E12S15, doi:10.1029/2006JE002791.

Morris, R. V., G. Klingelhöfer, C. Schröder, I. Fleischer, D. W. Ming, A. S. Yen, R. Gellert, R. E. Arvidson, D. S. Rodionov, L. S. Crumpler, B. C. Clark, B. A. Cohen, T. J. McCoy, D. W. Mittlefehldt, M. E. Schmidt, P. A. de Souza Jr., and S. W. Squyres (2008), Iron mineralogy and aqueous alteration from Husband Hill through Home Plate at Gusev Crater, Mars: Results from the Mössbauer instrument on the Spirit Mars Exploration Rover, *J. Geophys. Res.*, *113*, E12S42, doi:10.1029/2008JE003201.

Nehru, C. E., S. M. Zucker, and G. E. Harlow (1980), Olivines and olivine coronas in mesosiderites, *Geochim. Cosmochim. Acta, 44*, 1103– 1118.

Nittler, L. R., T. J. McCoy, P. E. Clark, M. E. Murphy, J. I. Trombka, and E. Jarosewich (2004), Bulk element compositions of meteorites: A guide for interpreting remote-sensing geochemical measurements of planets and asteroids, *Antarctic Meteorite Research, 17*, 231–251.

Petrovich, J. J. (2001), Review of the Mechanical Properties of Meteorites and their Constituents, *J. Mater. Sci.*, 36, 1579 – 1583.

Powell, B. N. (1970), Petrology and chemistry of mesosiderites-II. Silicate textures and compositions and metal-silicate relationships, *Geochim. Cosmochim. Acta, 35*, 5 – 34.

Prinz, M., C. E. Nehru, J. S. Delaney, and G. E. Harlow (1980), Modal studies of mesosiderites and related achondrites, including the new mesosiderite ALHA77219, *Proc. Lunar Planet. Sci. Conf. 11th*, 1055–1071.

Rieder, R., R. Gellert, J. Brückner, G. Klingelhöfer, G. Dreibus, A. Yen, and S. W. Squyres (2003), The new Athena alpha particle X-ray spectrometer for the Mars Exploration Rovers, *J. Geophys. Res.*, *108*(E12), 8066, doi:10.1029/2003JE002150.

Schröder, C., G. Klingelhöfer, and W. Tremel (2004), Weathering of Fe-bearing minerals under Martian conditions, investigated by Mössbauer spectroscopy, *Planet. Space Sci.*, *52*(11), 997-1010, doi:10.016/j.pss.2004.07.018.

Schröder, C., R. Gellert, B. L. Jolliff, G. Klingelhöfer, T. J. McCoy, R. V. Morris, D. S. Rodionov, P. A. de Souza Jr., A. S. Yen, J. Zipfel, and the Athena Science Team (2006), A stony meteorite discovered by the Mars Exploration Rover Opportunity on Meridiani Planum, Mars, *Meteorit. Planet. Sci.*, *41*, Supplement, A160.

Schröder, C., D. S. Rodionov, T. J. McCoy, B. L. Jolliff, R. Gellert, L. R. Nittler, W. H. Farrand, J. R. Johnson, S. W. Ruff, J. W. Ashley, D. W. Mittlefehldt, K. E. Herkenhoff, I. Fleischer, A. F. S. Haldemann, G. Klingelhöfer, D. W. Ming, R. V. Morris, P. A. de Souza Jr., S. W. Squyres, C. Weitz, A. S. Yen, J. Zipfel, and T. Economou (2008), Meteorites on Mars observed with the Mars Exploration Rovers, *J. Geophys. Res.*, *113*, E06S22, doi:10.1029/2007JE002990.

Schröder, C., J. W. Ashley, M. G. Chapman, B. A. Cohen, W. H. Farrand, I. Fleischer, R. Gellert, K. E. Herkenhoff, J. R. Johnson, B. L. Jolliff, J. Joseph, G. Klingelhöfer, R. V. Morris, S. W. Squyres, and S. P. Wright (2009a), Santorini, Another Meteorite on Mars and Third of a Kind, *Lunar Planet. Sci.*, *40*, 1665.

Schröder, C., J. W. Ashley, I. Fleischer, R. Gellert, G. Klingelhöfer, P. A. de Souza Jr., and the Athena Science Team (2009b), Meteorites on Mars: Implications from Three Probably Paired Meteorite Candidates at Meridiani Planum, *Meteorit. Planet. Sci., 44*, Supplement, A188.

Soderblom, L. A., R. C. Anderson, R. E. Arvidson, J. F. Bell III, N. A. Cabrol, W. Calvin, P. R. Christensen, B. C. Clark, T. Economou, B. L. Ehlmann, W. H. Farrand, D. Fike, R. Gellert, T. D. Glotch, M. P. Golombek, R. Greeley, J. P. Grotzinger, K. E. Herkenhoff, D. J. Jerolmack, J. R. Johnson, B. Jolliff, G. Klingelhöfer, A. H. Knoll, Z. A. Learner, R. Li, M. C. Malin, S. M. McLennan, H. Y. McSween, D. W. Ming, R. V. Morris, J. W. Rice Jr., L. Richter, R. Rieder, D. Rodionov, C. Schröder, F. P. Seelos IV, J. M. Soderblom, S. W. Squyres, R. Sullivan, W. A. Watters, C. M. Weitz, M. B. Wyatt, A. Yen, and J. Zipfel (2004), Soils of Eagle Crater and Meridiani Planum at the Opportunity Rover Landing Site, *Science, 306*, 1723-1726, http://dx.doi.org/10.1126/science.1105127.

Squyres, S. W., R. E. Arvidson, E. T. Baumgartner, J. F. Bell III, P. R. Christensen, S. Gorevan, K. E. Herkenhoff, G. Klingelhöfer, M. B. Madsen, R. V. Morris, R. Rieder, and R. A. Romero (2003), Athena Mars rover science investigation, *J. Geophys. Res., 108*(E12), 8062, doi:10.1029/2003JE002121.

Squyres, S. W., R. E. Arvidson, J. F. Bell III, J. Brückner, N. A. Cabrol, W. Calvin, M. H. Carr, P. R. Christensen, B. C. Clark, L. Crumpler, D. J. Des Marais, C. D'Uston, T. Economou, J. Farmer, W. Farrand, W. Folkner, M. Golombek, S. Gorevan, J. A. Grant, R. Greeley, J. Grotzinger, L. Haskin, K. E. Herkenhoff, S. Hviid, J. Johnson, G. Klingelhöfer, A. H. Knoll, G. Landis, M. Lemmon, R. Li, M. B. Madsen, M. C. Malin, S. M. McLennan, H. Y. McSween, D. W. Ming, J. Moersch, R. V. Morris, T. Parker, J. W. Rice Jr., L. Richter, R.

Rieder, M. Sims, M. Smith, P. Smith, L. A. Soderblom, R. Sullivan, H. Wänke, T. Wdowiak, M. Wolff, and A. Yen (2004), The Opportunity Rover's Athena Science Investigation at Meridiani Planum, Mars, *Science, 306*, 1698-1703.

Squyres, S. W., A. H. Knoll, R. E. Arvidson, B. C. Clark, J. P. Grotzinger, B. L. Jolliff, S. M. McLennan, N. Tosca, J. F. Bell III, W. M. Calvin, W. H. Farrand, T. D. Glotch, M. P. Golombek, K. E. Herkenhoff, J. R. Johnson, G. Klingelhöfer, H. Y. McSween, and A. S. Yen (2006a), Two Years at Meridiani Planum: Results from the Opportunity Rover, *Science, 313*, 1403-1407, doi:10.1126/science.1130890.

Squyres, S. W., R. E. Arvidson, D. Bollen, J. F. Bell III, J. Brückner, N. A. Cabrol, W. M. Calvin, M. H. Carr, P. R. Christensen, B. C. Clark, L. Crumpler, D. J. Des Marais, C. d'Uston, T. Economou, J. Farmer, W. H. Farrand, W. Folkner, R. Gellert, T. D. Glotch, M. Golombek, S. Gorevan, J. A. Grant, R. Greeley, J. Grotzinger, K. E. Herkenhoff, S. Hviid, J. R. Johnson, G. Klingelhöfer, A. H. Knoll, G. Landis, M. Lemmon, R. Li, M. B. Madsen, M. C. Malin, S. M. McLennan, H. Y. McSween, D. W. Ming, J. Moersch, R. V. Morris, T. Parker, J. W. Rice Jr., L. Richter, R. Rieder, C. Schröder, M. Sims, M. Smith, P. Smith, L. A. Soderblom, R. Sullivan, N. J. Tosca, H. Wänke, T. Wdowiak, M. Wolff, and A. Yen (2006b), Overview of the Opportunity Mars Exploration Rover Mission to Meridiani Planum: Eagle Crater to Purgatory Ripple, *J. Geophys. Res., 111*, E12S12, doi:10.1029/2006JE002771.

Squyres, S. W., A. H. Knoll, R. E. Arvidson, J. W. Ashley, J. F. Bell III, W. M. Calvin, P. R. Christensen, B. C. Clark, B. A. Cohen, P. A. de Souza Jr., L. Edgar, W. H. Farrand, I. Fleischer, R. Gellert, M. P. Golombek, J. Grant, J. Grotzinger, A. Hayes, K. E. Herkenhoff, J. R. Johnson, B. Jolliff, G. Klingelhöfer, A. Knudson, R. Li, T. McCoy, S. M. McLennan, D. W. Ming, D. W. Mittlefehldt, R. V. Morris, J. W. Rice Jr., C. Schröder, R. J. Sullivan, A.

Yen, and R. A. Yingst (2009), Exploration of Victoria Crater by the Mars Rover Opportunity, *Science*, *324*, 1058-1061, doi:10.1126/science.1170355.

Wilkison, S. L., and M. S. Robinson (2000), Bulk density of ordinary chondrite meteorites and implications for asteroidal internal structure, *Meteorit. Planet. Sci.*, *35*, 1203– 1213.

Figure Captions

Figure 1 – False color Pancam images of the candidate stony meteorites a) Barberton, b) Santa Catarina, c) Santorini and d) Kasos. White boxes indicate locations of MI/Pancam false-color merges shown in Figures 3-6.

Figure 2 – Opportunity's traverse and locations of meteorite finds. Map based on rover positioning data by *Li et al.* [2010].

Figure 3 – Merge of calibrated MI image 1M139013191IFF2809P2956M2F1 of Barberton, acquired on Sol 122 when target was partly shadowed, with calibrated Pancam color images acquired on Sol 123 by sequence p2535.

Figure 4 – Merge of mosaic of calibrated MI images of Santa Catarina, acquired on Sol 1045 when target was fully shadowed, with calibrated Pancam color images acquired on Sol 1055 by sequence p2564.

Figure 5 – Merge of mosaic of calibrated MI images of Santorini, acquired on Sol 1747 when the target was illuminated from the upper right, with calibrated Pancam color images acquired on Sol 1748 by sequence p2597.

Figure 6 – Merge of mosaic of calibrated MI images of Kasos, acquired on Sol 1886 when the target was illuminated from the top, with calibrated Pancam color images acquired on Sol 1884 by sequence p2574.

Figure 7 – Chemical compositions of ‘cobbles’ at Meridiani Planum normalized to standard Meridiani S-rich outcrop. Barberton, Santa Catarina, Santorini, and Kasos are a group distinct on the basis of their chemical composition [cf. *Fleischer et al.*, 2010c].

Figure 8 – Mössbauer spectra showing Fe mineral subspectral areas (compaer to Table 2) for Barberton, Santa Catarina, Santorini, and Kasos.

Figure 9 – Element ratio plots for classification of candidate stony meteorites after *Nittler et al.* [2004]. Figure taken from *Schröder et al.* [2008] and updated with values for Santorini and Kasos. Original and soil-subtracted values (Table 1) are given for Barberton. Shergottites include members from the subgroups of basaltic shergottites (Shergotty, Zagami, and EET 79001, lithology B), olivine-phyric shergottites (EET 79001, litology A), and lherzolitic shergottites (ALH 77005).

Figure 10 - A plot of the relative landing rates of 0.1 - 10 kg stony meteorites vs. entry velocity and entry angle. The units are arbitrary. For a 6 mbar atmosphere, meteorite landing is limited to entry angles of 7° - 39° and velocities less than ~17 km s^{-1}. It is maximized for entry angles of ~22° and a velocity of ~6 km s^{-1}, which is the theoretical minimum for Mars.

Figure 11 – Meteorite finds in relation to Victoria crater. Victoria crater has a diameter of ~800 m (radius of ~400 m). Radii of concentric circles increase in 400 m increments. Map based on rover positioning data by *Li et al.* [2010].

Figure 12 – Map of meteorite fragment finds around Barringer Meteor Crater in Arizona. Note that each circle represents a one mile increment from the crater rim. Figure taken with permission from *Kring* [2007].

Table 1. **Elemental composition of candidate meteorites.**

	Barberton	Barberton minus soil		Santa Catarina	Santorini 1	Santorini 2	Kasos
		25 %[a]	35 %[a]				
	[wt%]	[wt%]	[wt%]	[wt%]	[wt%]	[wt%]	[wt%]
SiO_2	44.3 ± 0.51	44.0	43.8	44.0 ± 0.41	44.1 ± 0.42	44.7 ± 0.50	43.7 ± 0.29
TiO_2	0.51 ± 0.07	0.35	0.26	0.24 ± 0.06	0.31 ± 0.06	0.23 ± 0.06	0.23 ± 0.06
Al_2O_3	6.20 ± 0.18	5.19	4.58	4.35 ± 0.10	4.43 ± 0.10	3.93 ± 0.09	4.27 ± 0.08
FeO[b]	19.8 ± 0.17	20.5	21.0	20.6 ± 0.13	22.1 ± 0.14	20.9 ± 0.14	21.0 ± 0.08
MnO	0.36 ± 0.02	0.36	0.36	0.38 ± 0.01	0.37 ± 0.01	0.39 ± 0.01	0.39 ± 0.01
MgO	14.79 ± 0.23	17.2	18.7	18.04 ± 0.20	17.79 ± 0.19	19.67 ± 0.21	18.25 ± 0.15
CaO	4.42 ± 0.06	3.65	3.17	3.43 ± 0.03	3.26 ± 0.03	2.92 ± 0.03	3.00 ± 0.03
Na_2O	1.76 ± 0.34	1.55	1.43	1.51 ± 0.35	1.50 ± 0.33	1.43 ± 0.36	1.59 ± 0.20
K_2O	0.29 ± 0.06	0.22	0.17	0.14 ± 0.05	0.14 ± 0.05	0.11 ± 0.05	0.15 ± 0.05
P_2O_5	0.66 ± 0.09	0.59	0.55	0.61 ± 0.07	0.59 ± 0.07	0.54 ± 0.07	0.55 ± 0.07
Cr_2O_3	0.50 ± 0.04	0.55	0.58	0.61 ± 0.04	0.61 ± 0.04	0.62 ± 0.04	0.55 ± 0.03
Cl	0.60 ± 0.02	0.52	0.47	0.62 ± 0.01	0.53 ± 0.01	0.51 ± 0.01	0.43 ± 0.01
SO_3[c]	5.56 ± 0.11	5.05	4.73	5.09 ± 0.07	3.88 ± 0.06	3.40 ± 0.06	5.50 ± 0.06
	[ppm]	[ppm]	[ppm]	[ppm]	[ppm]	[ppm]	[ppm]
Ni	1639 ± 89	2018	2251	3207 ± 76	3255 ± 76	4979 ± 91	2722 ± 65
Zn	207 ± 25	151	116	164 ± 13	128 ± 12	120 ± 12	88 ± 9
Br	47 ± 21	51	53	59 ± 16	22 ± 15	20 ± 15	99 ± 15

[a]Values adapted from *Schröder et al.* [2008].

[b]Total Fe expressed as oxide for comparison only. Some of the Fe is present as Fe^0 (kamacite) or Fe^{3+}.[c]Total S expressed as oxide for comparison only. Some or most of the S in Barberton is likely reduced and present as sulfide (troilite).

Table 2. Mössbauer subspectral areas of Fe-bearing minerals in candidate meteorites.

Rock	Olivine Fe^{2+} %[a]	Pyroxene Fe^{2+} %	npOx Fe^{3+} %	Kamacite Fe^{0} %	Troilite Fe^{2+} %
Barberton	48	32	6	11	3
Santa Catarina	52	26	14	1	6
Santorini	53	28	8	2	9
Kasos	32	41	8	5	14

[a]Uncertainty for area ratios is ±2 % absolute for Barberton, Santa Catarina, and Santorini, and ±4 % for Kasos.

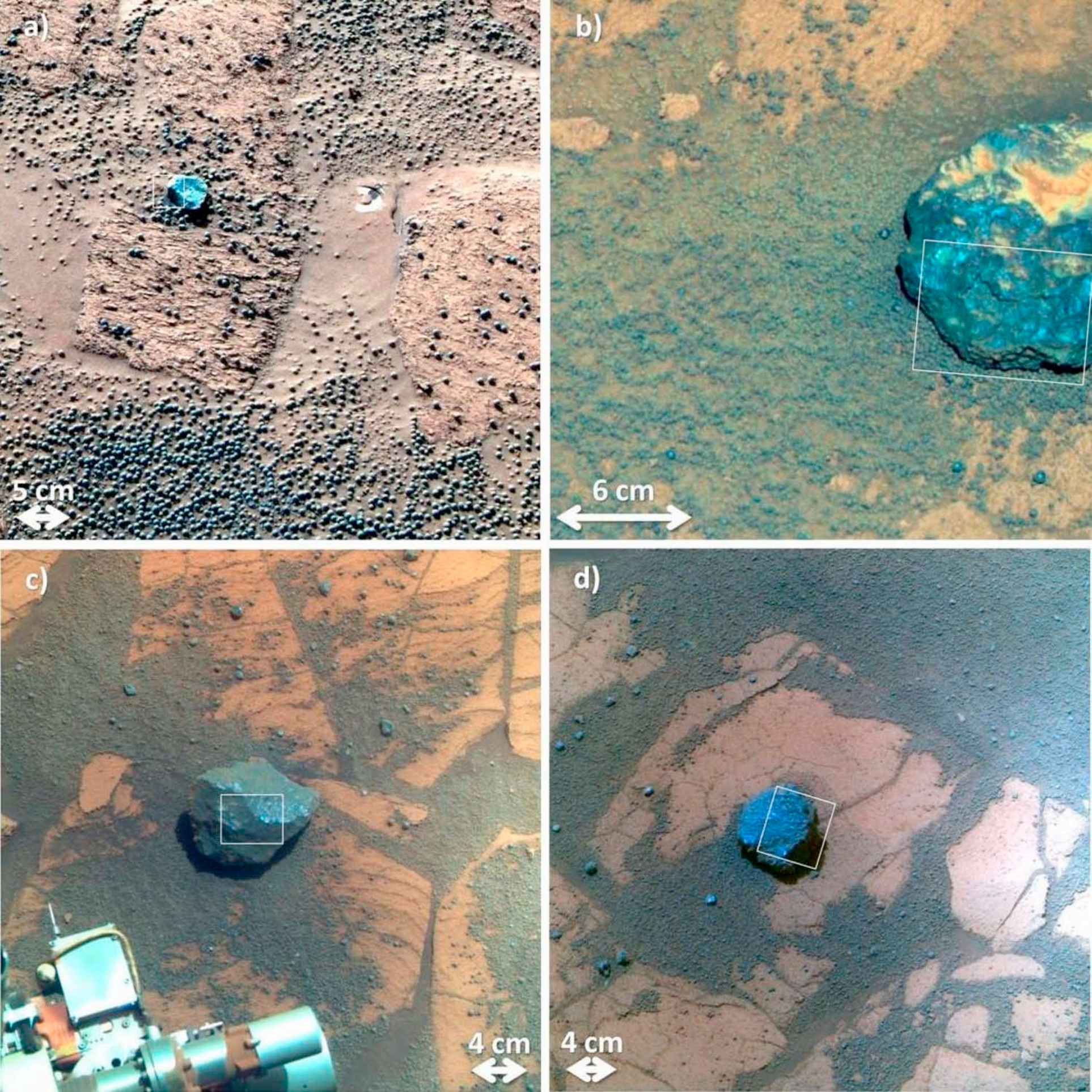
a)
5 cm
b)
6 cm
c)
4 cm
d)
4 cm

Opportunity Traverse Map (Sol 2063)

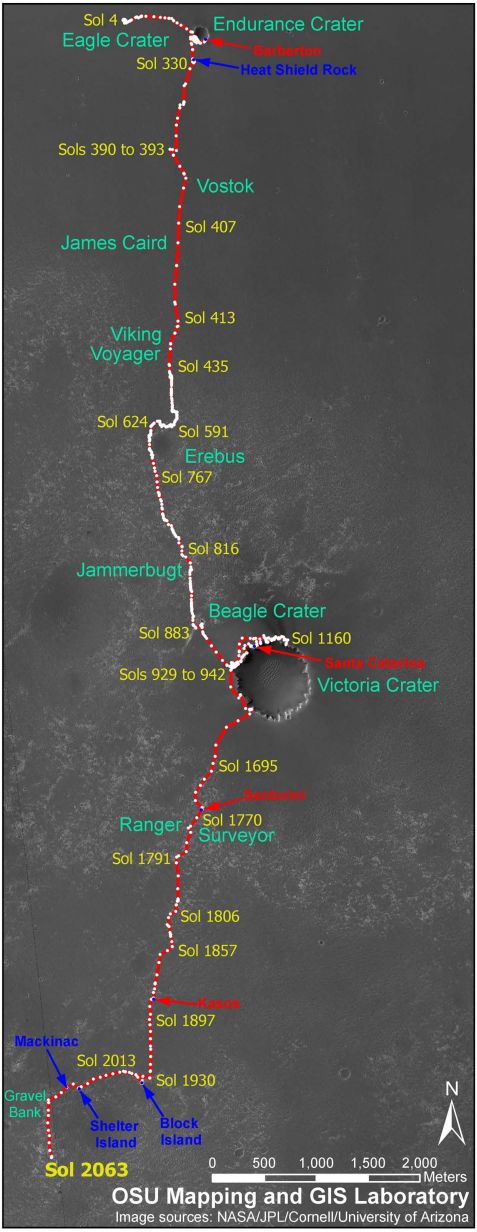

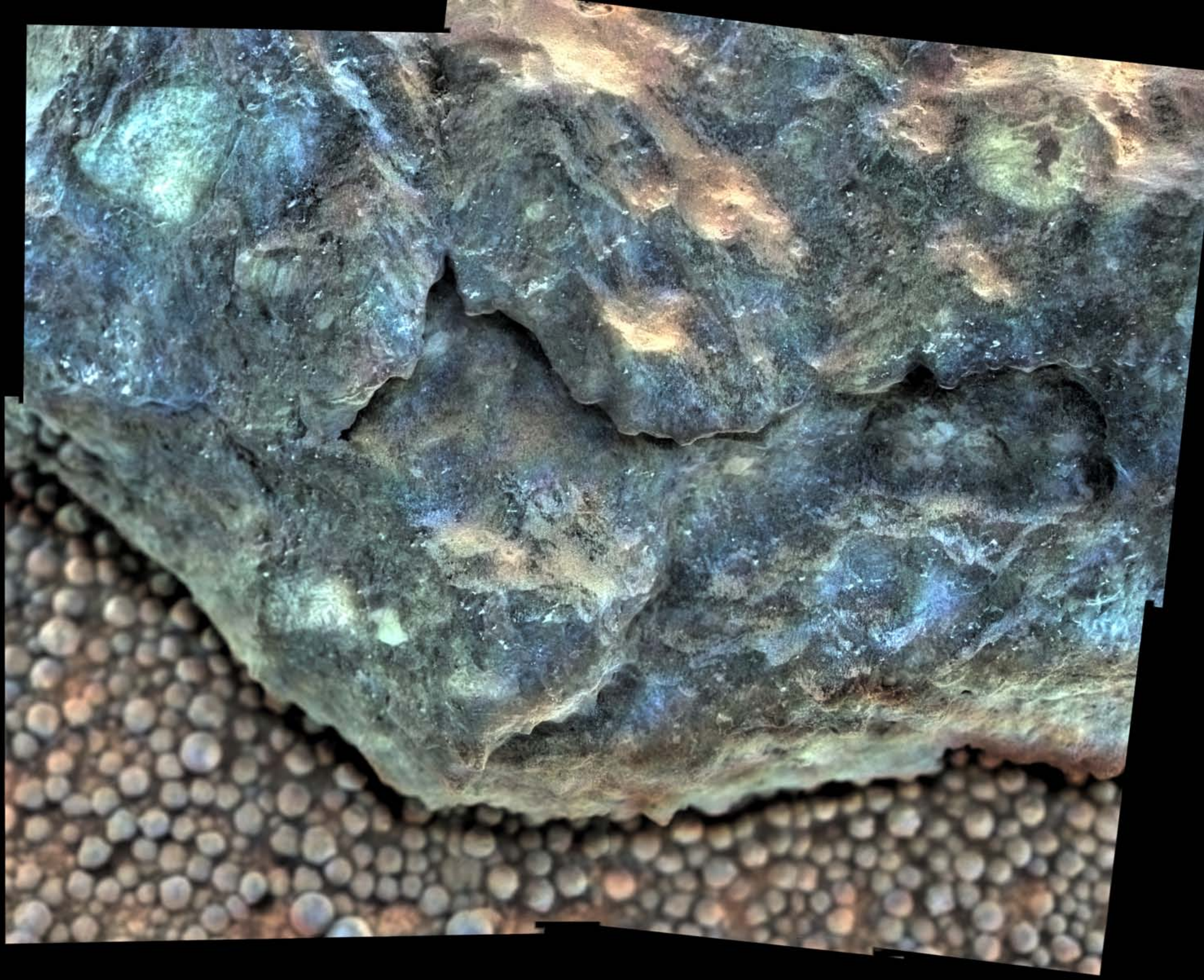

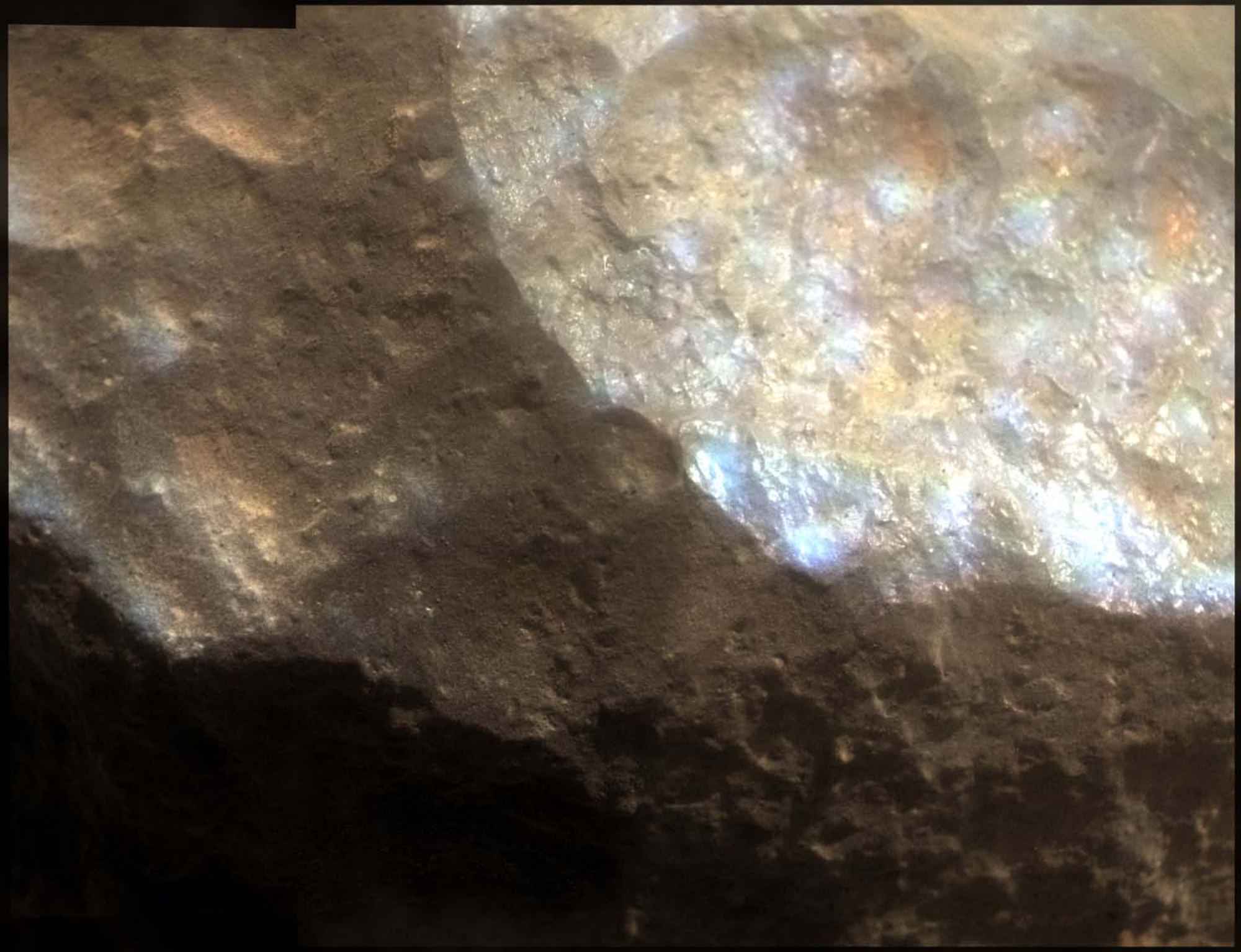

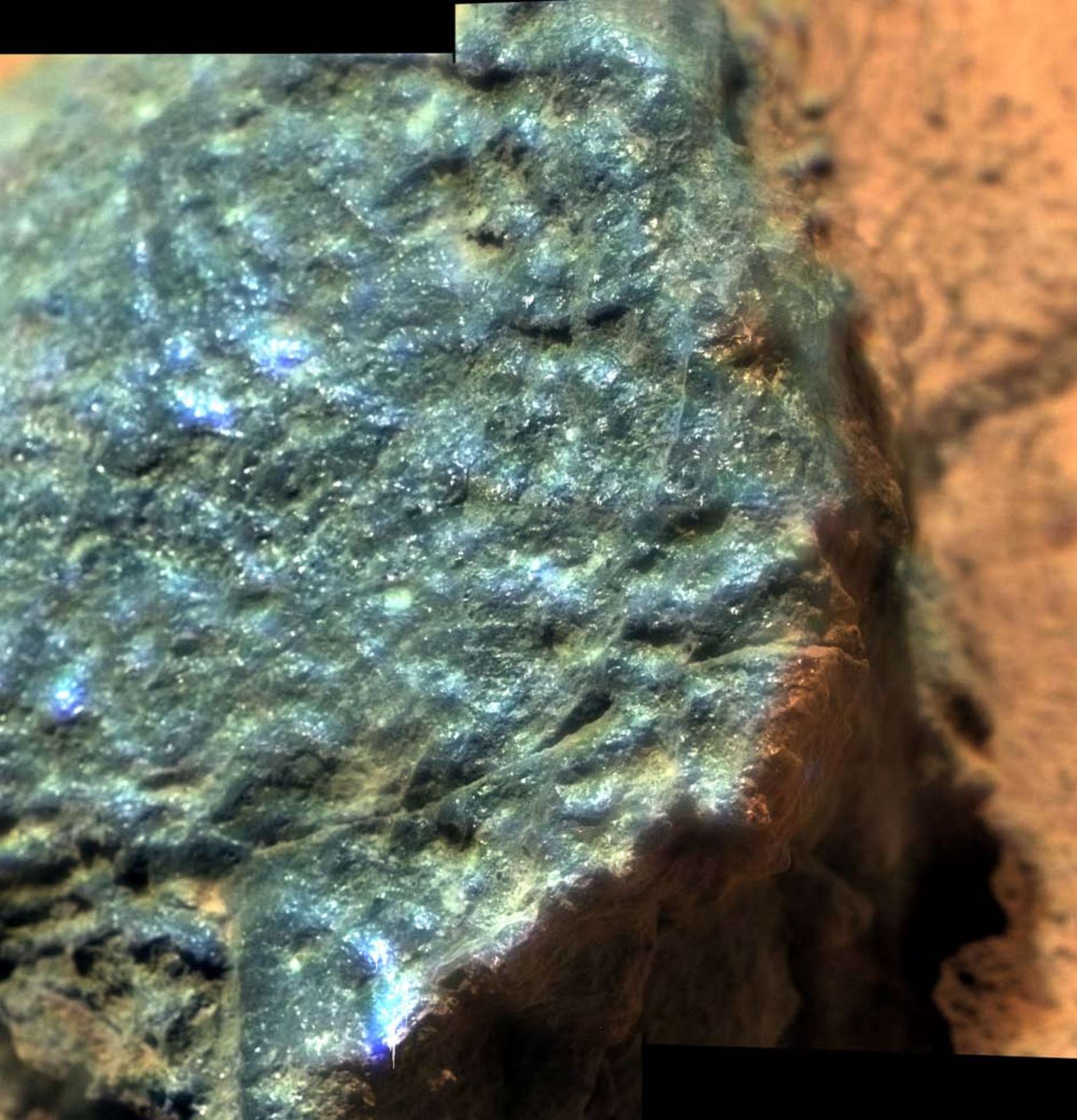

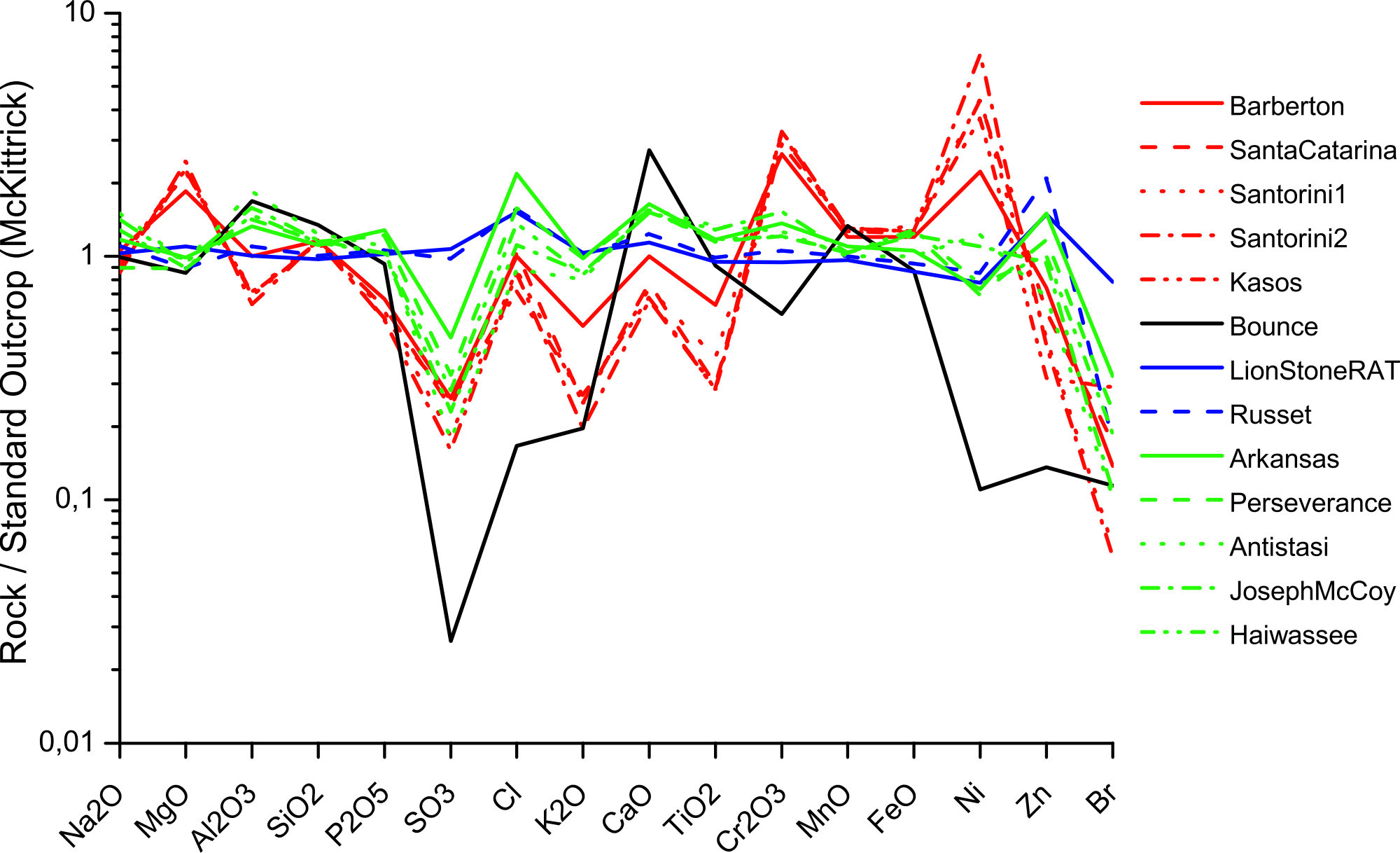
Rock / Standard Outcrop (McKittrick)
10
1
0,1
0,01
Na2O
MgO
Al2O3
SiO2
P2O5
SO3
Cl
K2O
CaO
TiO2
Cr2O3
MnO
FeO
Ni
Zn
Br
Barberton
SantaCatarina
Santorini1
Santorini2
Kasos
Bounce
LionStoneRAT
Russet
Arkansas
Perseverance
Antistasi
JosephMcCoy
Haiwassee

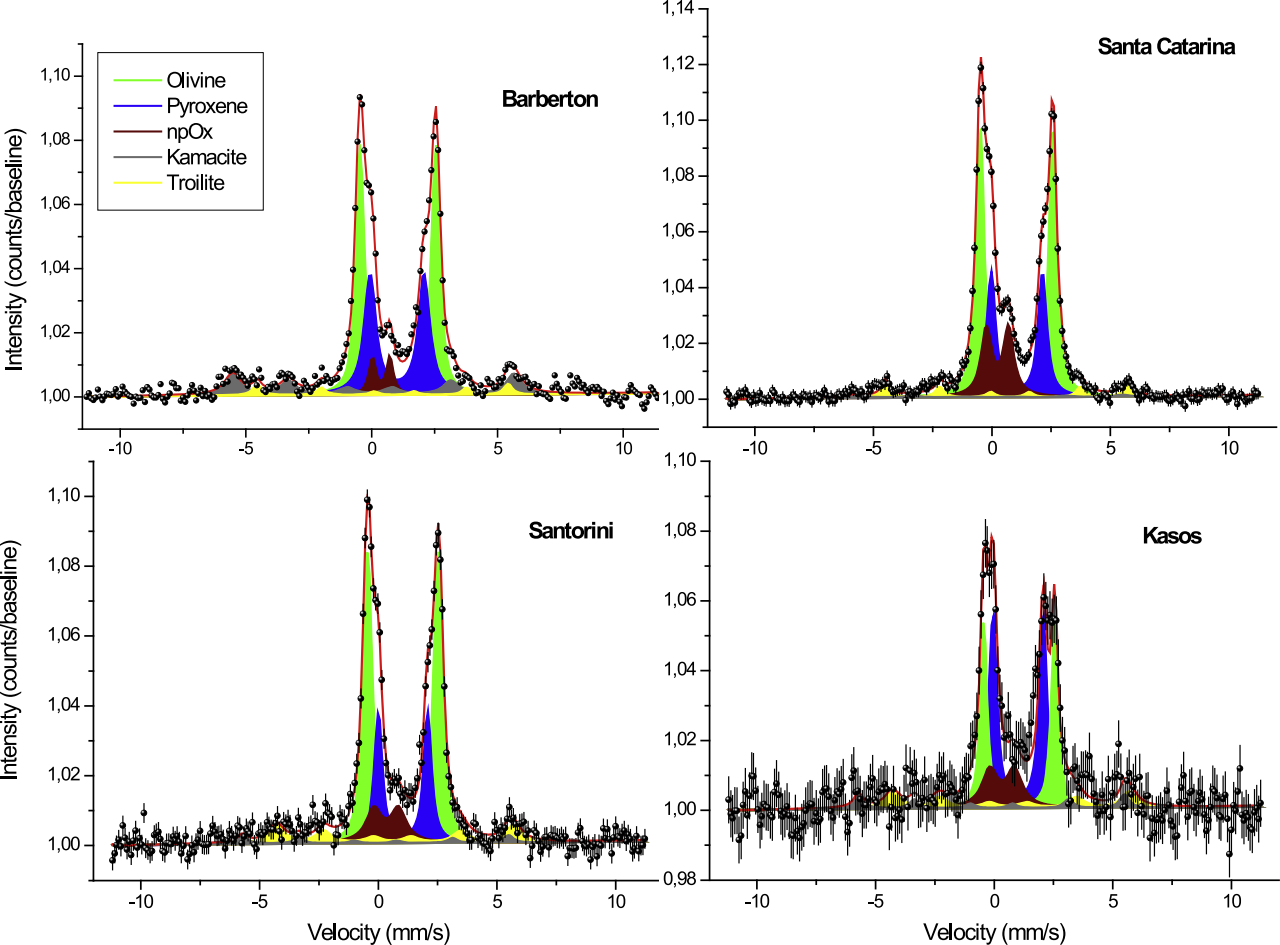
Olivine
Pyroxene
npOx
Kamacite
Troilite
Barberton
Santa Catarina
Santorini
Kasos
Intensity (counts/baseline)
Velocity (mm/s)
1,14
1,12
1,10
1,08
1,06
1,04
1,02
1,00
0,98
-10
-5
0
5
10

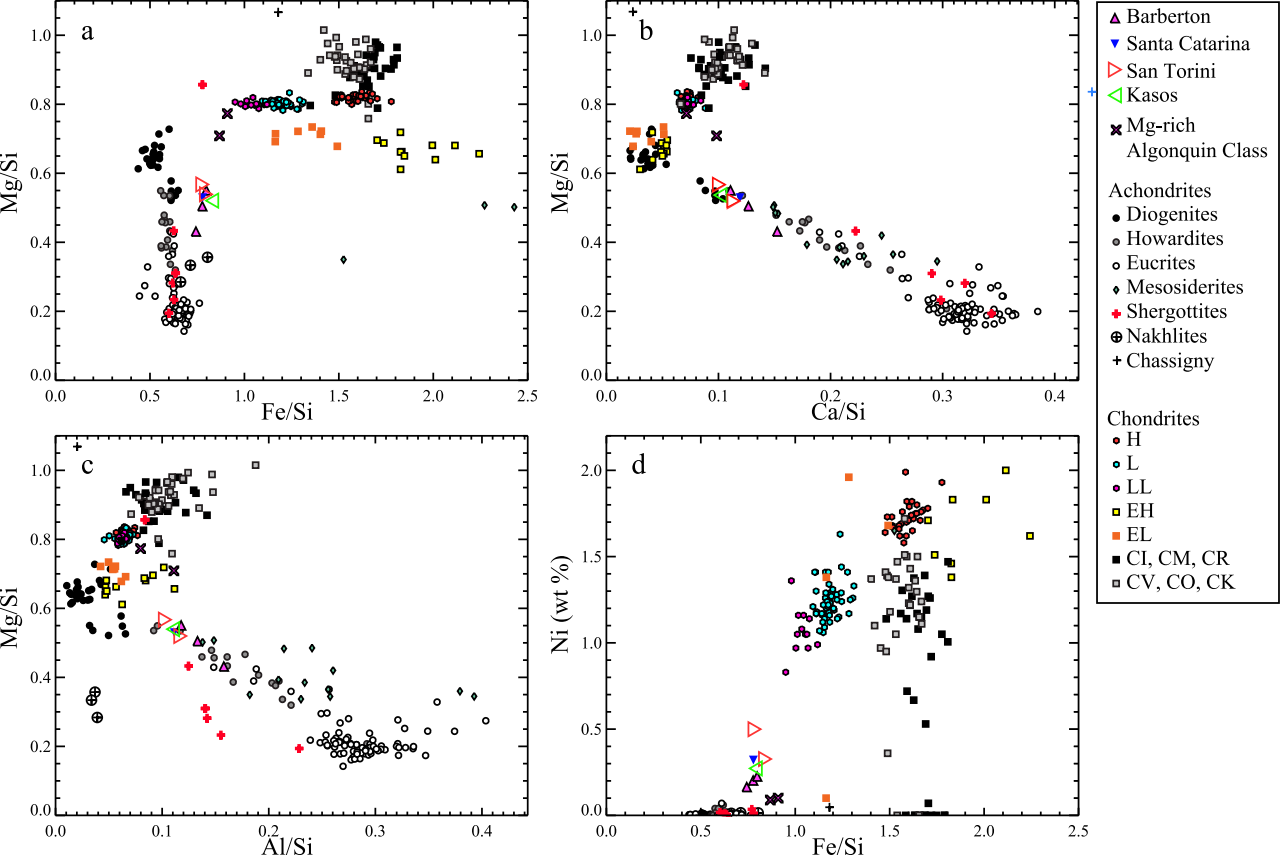
a
b
c
d
Mg/Si
Fe/Si
Ca/Si
Al/Si
Ni (wt %)
Barberton
Santa Catarina
San Torini
Kasos
Mg-rich Algonquin Class
Achondrites
Diogenites
Howardites
Eucrites
Mesosiderites
Shergottites
Nakhlites
Chassigny
Chondrites
H
L
LL
EH
EL
CI, CM, CR
CV, CO, CK

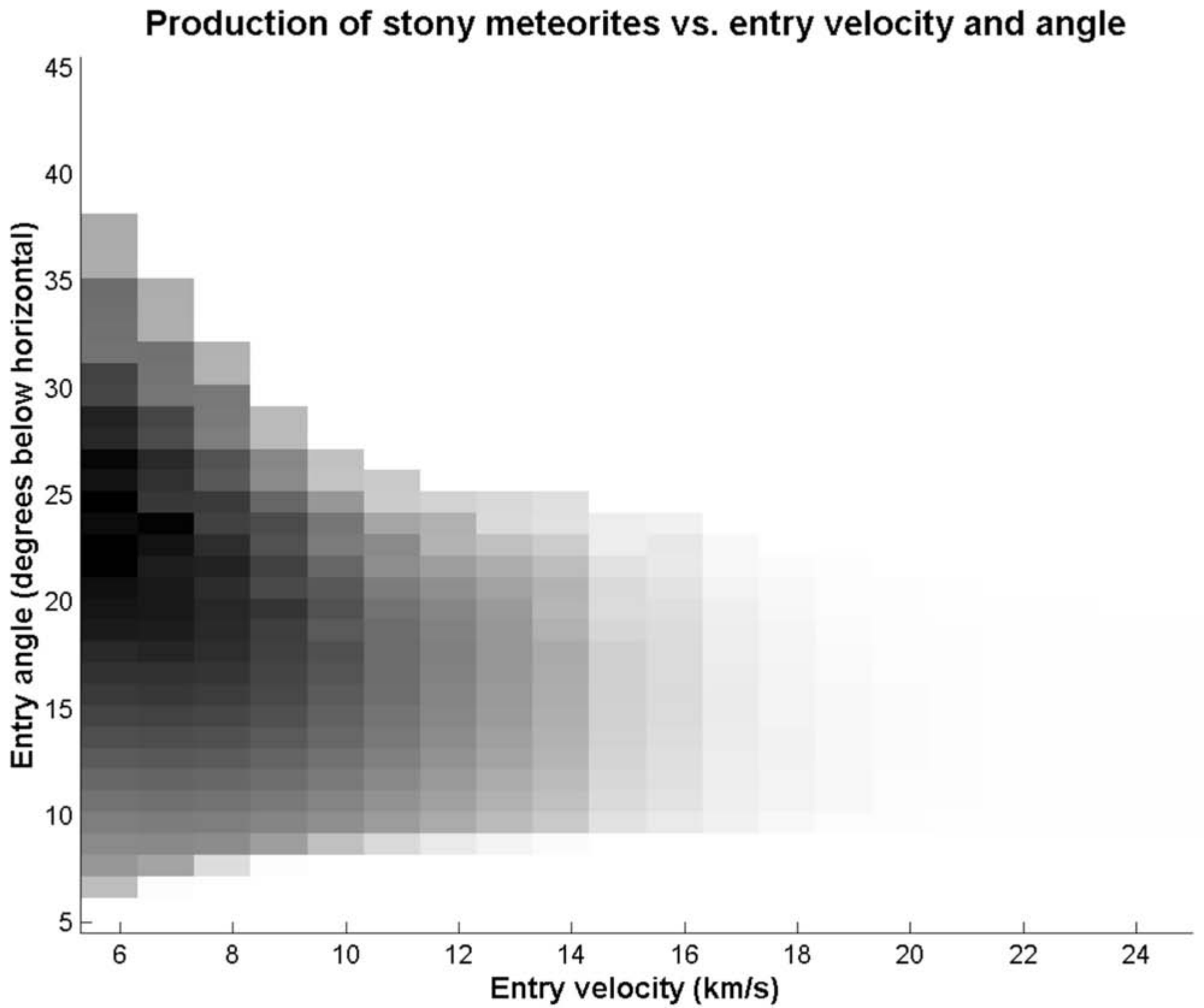
Production of stony meteorites vs. entry velocity and angle
Entry angle (degrees below horizontal)
45
40
35
30
25
20
15
10
5
6
8
10
12
14
16
18
20
22
24
Entry velocity (km/s)

Opportunity Traverse Map (Sol 2063)

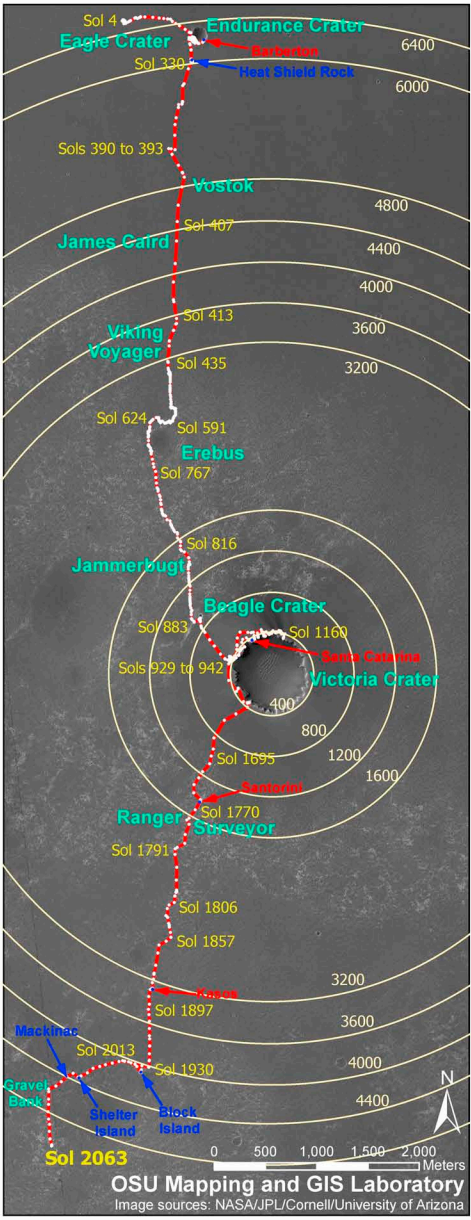

Distribution of Meteoritic Material Around Meteor Crater, Coconino Co., Arizona

Reproduced from November 1908 map published by Barringer (1910).

Legend

- Canyon Diablo iron meteorites from 10 to 547 lbs. Discovered by Standard Iron Company.
- Canyon Diablo iron meteorites from 10 to 1000 lbs. Discovered by employees of F.W. Volz et al., previous to acquisition of property by S.I.Co.
- Small Canyon Diablo iron meteorites. Discovered by S.I.Co. The distribution of specimens is only approximated because thousands were found. Specimens are usually a few grains or ounces in weight; irons weighing from 1 to 10 lbs were only found occasionally.
- Large irregular masses of meteoritic iron oxide or large shale balls from 100 to 300 lbs in weight, due to oxidation of meteoritic iron rich in chlorine and sulphur or shale ball iron.
- Small broken fragments of meteoritic iron oxide or iron shale (a few grains or ounces, rarely a pound in weight). Thousands of such pieces found, hence distribution only approximated.